J|A|C|S
COMMUNICATIONS

Templating Odd Numbered Magnetic Rings: Oxovanadium Heptagons Sandwiched by β-Cyclodextrins

Norihisa Hoshino,[†] Motohiro Nakano,[‡] Hiroyuki Nojiri,[§] Wolfgang Wernsdorfer,[¶] and Hiroki Oshio*,[†]

Graduate School of Pure and Applied Sciences, University of Tsukuba, Tennodai 1-1-1, Tsukuba 305-8571, Japan, Department of Applied Chemistry, Graduate School of Engineering, Osaka University, Yamadaoka 2-1, Suita, Osaka 565-0871, Japan, Institute of Material Research, Tohoku University, Katahira 2-1-1, Aoba-ku, Sendai 980-8577, Japan, and Institut Néel, CNRS & Université J. Fourier, BP 166, 25 rue des Martyrs, 38042 GRENOBLE Cedex 9, France

Received August 5, 2009; E-mail: oshio@chem.tsukuba.ac.jp

Molecules exhibit chemical and physical properties characteristic of their molecular shapes and the number of constituents, and odd/even-membered effects have fascinated scientists for decades, such as in the oscillating melting temperatures in a series of *n*-alkane crystals (C_nH_{2n+2})[1] and as in the spin gap of spin ladders with odd-numbered legs.[2] Similarly, paramagnetic ring-shaped molecules are expected to exhibit magnetism dependent upon the number of constituent metal ions. Even-membered antiferromagnetic rings, in which neighboring spins have opposite orientation (up and down spins), have singlet ground states and may exhibit quantum rotation of the Néel vector.[3] In odd-membered rings, all spins cannot be aligned in an alternating fashion and the residual spin can have any orientation, resulting in a spin frustrated system. Antiferromagnetic odd-membered rings have a periodic spin behavior involving the spin phase inversion.[4] Since a detailed magnetic study was completed on a decanuclear ferric wheel,[5] several even-membered rings have been reported. However, odd-membered systems of more than three members have only rarely been described, such as in $[(C_6H_{11})_2NH_2][Cr_8NiF_9(O_2CCMe_3)_{18}]$[4] and $La(NO_3)_3[15\text{-}MC_{Cu(II)N(picha)}\text{-}5]$ (H_2picha = picoline hydroxamic acid),[6] and the magnetism of homometal odd-membered rings has yet to be explored. The lack of examples may be due to kinetic and thermodynamic issues, as well as the lack of crystallographic odd-number-fold rotational symmetries higher than three. To circumvent this problem, we set out to utilize cyclodextrin (CD)-based template systems. Recently, Klüfers et al. reported an oxovanadate complex of $Na_6[VO_6Na_6(\alpha\text{-}CDH_{12})_2]\cdot 59H_2O$, in which two α-CD molecules sandwich six oxovanadium ions; however, its magnetic properties have not been studied.[7] This result prompted us to target the assembly of a seven-membered ring using β-CD as a template, and herein we report the syntheses and magnetism of an unprecedented heptanuclear oxovanadium ring.

The reaction of $V{=}O(SO_4)_2\cdot nH_2O$ with β-CD and NaOH in water yielded a green solution, and the resulting solution was dispersed with acetone and methanol to give blue hexagonal rods and blue plates of $Na_7[(V{=}O)_7Na_7(H_2O)_7(\beta\text{-}CD)_2]\cdot nH_2O$ (**1**) and (**2**) with yields of 38 and 47%, respectively. **1** and **2** crystallized in the trigonal *R*32 and monoclinic $P2_1$ space groups, respectively (Figure 1). The complex molecule in **1** has C_2 symmetry, while the oxovanadium ions in **2** are crystallographically independent. Subtle differences in ring distortion result in characteristic magnetic behavior in each. The core structures of the complex anions in **1** and **2** can be described as cyclic heptagons of oxovanadium (V═O) ions where the cyclic core is sandwiched between two β-CDs. β-CD has 7 primary and 14 secondary alcohol groups. All secondary alcohols are deprotonated to bridge the vanadium and sodium ions, while the primary alcohols remain protonated. The selected interatomic bonds distances and angles were summarized in Figure 1S. In the ring, the vanadium and sodium ions are doubly bridged by hydroxyl groups of β-CD; hence, the neighboring vanadium ions are separated by O−Na−O groups. The neighboring vanadium ions in the rings are separated by 6.197(3)−6.3961(19) Å and 6.360(3)−6.450(3) Å in **1** and **2**, respectively. The interior angles of the vanadyl heptagon are in the range of 125.76(2)°−130.097(15)° and 126.19(4)°−130.96(3)°, respectively, for **1** and **2**, which are close to the value (128.57°) expected for the regular heptagon. The coordination geometry of the vanadium ions is square pyramidal. The basal sites are coordinated by oxygen atoms from secondary alcohols with bond lengths of V−O = 1.915(4)−2.013(4) Å and 1.893(8)−2.027(10) Å for **1** and **2**, respectively, and the axial sites are occupied by the oxyl ions with bond lengths of 1.575(6)−1.629(6) Å and 1.613(7)−1.684(8) Å, respectively. The coordination geometry of the sodium ions in the ring is square pyramidal, where four alkoxo-oxygen atoms from β-CD occupy the basal positions and a water molecule coordinates in the axial site.

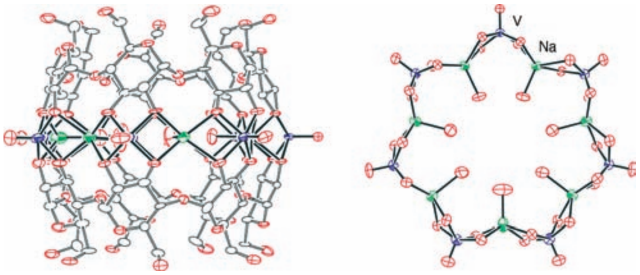

Figure 1. Sandwich structure of an oxovanadium heptagon (left) and its core structure without cyclodextrins (right).

Magnetic susceptibility data for **1** and **2** were collected on microcrystalline samples in the temperature range 1.8 − 300 K in an applied field of 1 T, and the data obeyed the Curie−Weiss law with $C = 2.37$ emu mol^{-1} K and $\theta = -0.34$ K for **1** and $C = 2.36$ emu mol^{-1} K and $\theta = -0.53$ K for **2** (Figure 2S). Low temperature magnetization experiments were carried out on single crystals at 0.04−0.9 K by using a microsquid technique. Temperature variations of *M* versus *H* plots are depicted in Figure 2 for **1** and Figure 3S for **2**, together with d*M*/d*H* versus *H* plots. When the temperatures were higher than 0.25 K, the *M* values increased monotonically as the magnetic field was increased; however, the *M* versus *T* plots clearly showed stepped curves below 0.1 K.

[†] University of Tsukuba.
[‡] Osaka Universtiy.
[§] Tohoku University.
[¶] Institute Néel-CNRS.

10.1021/ja9066496 CCC: $40.75 © 2009 American Chemical Society

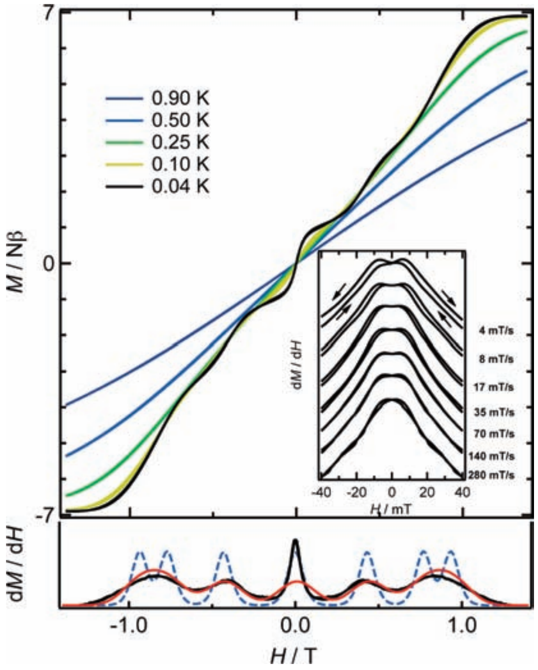

Figure 2. Magnetization (M) vs field (H) plots at 0.04−0.90 K (top) and the field derivatives (dM/dH) vs H plot at 0.04 K (bottom) for **1**, respectively. The black, blue dashed, and red curves in the dM/dH vs H plots correspond to the observed data, the simulation curves with the J values, and the hyperfine field of the vanadium nuclei, respectively. (inset) dM/dH vs H plots for several sweep rates (4−280 mT/s) at 0.04 K.

Magnetization of **1** reached the saturation value ($M_s = 6.90$ Nβ with $g = 1.973$) expected for $S = {}^7/_2$ at 1.2 T, while that for **2** did not reach saturation up to 1.4 T. The results clearly showed the presence of ground spin-level crossings at several magnetic fields induced by the Zeeman effect, and the stepped-shapes reflect the different antiferromagnetic interactions in **1** and **2**.

The magnetization data were analyzed using the Heisenberg−Dirac−van Vleck (HDVV) spin Hamiltonian including isotropic exchange interactions and the Zeeman term,

$$\hat{H} = -2\sum_{i=1}^{6}(J_i\hat{s}_i\cdot\hat{s}_{i+1}) - 2J_7\hat{s}_7\cdot\hat{s}_1 + g\beta\mu_0\sum_i \hat{S}_i\cdot\hat{H}$$

where J_i denotes exchange coupling constants between neighboring vanadium ions in the ring. Note that the vanadium ions have $S = {}^1/_2$ spin ground states and were treated as magnetically isotropic ions. Single crystal EPR spectra were measured for **1** and **2** with frequencies of 95−190 GHz at 4.2 K, which gave the isotropic g-values of 1.973 and 1.975, respectively (Figure 4S). The molecular rings are not regular heptagons, and the ring symmetries should be considered in the analyses of the magnetization data. The complex molecule of **1** has a crystallographic C_2 axis; hence, three exchange parameters of J_1 ($= J_3 = J_5 = J_7$), J_2 ($= J_6$), and J_4 were used (Figure 5S). The vanadyl ions in **2** are crystallographically independent; however, all vanadyl ions are located on almost the same plane, and the intervanadyl distances between some vanadyl pairs are similar. Four exchange parameters of J_1 ($= J_6$), J_2 ($= J_7$), J_3 ($= J_4$), and J_5 were, therefore, assumed (Figure 5S). Least square calculations yielded $J_1 = -0.31$ K, $J_2 = -0.26$ K, and $J_4 = -0.39$ K for **1** and $J_1 = -0.32$ K, $J_2 = -0.16$ K, $J_3 = -0.30$ K, and $J_5 = -0.60$ K for **2**. The magnetization curves calculated using the obtained J values reproduced the seven crossover fields of the lowest Zeeman split sublevels (m_s) of the four spin states ($S = {}^1/_2, {}^3/_2, {}^5/_2$, and ${}^7/_2$). The observed curves were broader than the simulated ones (blue lines in Figures 2 and 3S (bottom)), so a line-width function due to the nuclear hyperfine field was considered in the calculations, and the A_{iso} was set to 15 mT for each vanadium ion ($I = {}^7/_2$).[8] The results reproduced the observed dM/dH versus H curves for **1** and **2** (the red lines in Figures 2 and 2S). Note that the introduction of anisotropic exchange interactions in the calculations did not improve the fits.

The spin ground states ($S = {}^1/_2$) of an antiferromagnetic odd-membered ring are doubly degenerate because of the spin chirality. The degeneracy is lifted by the distortion of the heptagon, leading to the two Kramers' doublets with a very small gap. Two split peaks in the dM/dH vs H plots were observed around $H = 0$ T in **1** and **2** (Figures 2 and 3S inset). Supposing the peak maxima correspond to the level-crossing fields of the Zeeman-split sublevels, the peak separations (0.008 and 0.022 mT for **1** and **2**) correspond to energy gaps of 2.6 and 7.1 mK for **1** and **2**, respectively. The larger energy gap for **2** is in good accord with the more-distorted ring in **2**.

In conclusion, we have demonstrated the magnetism of antiferromagnetic seven-membered rings. The heptagons have two nearly degenerate $S = {}^1/_2$ spin ground states, and the energy gaps depend upon ring distortions. Magnetization experiments at 40 mK showed stepped magnetization curves, characteristic of Zeeman-level crossings in the heptagons.

Acknowledgment. This work was supported by a Grant-in-Aid for Scientific Research from the Ministry of Education, Culture, Sports, Science and Technology, Japan.

Supporting Information Available: Synthetic details, magnetic and EPR data of **1** and **2**. Single crystal X-ray data and CIF files for **1** and **2**. This material is available free of charge via the Internet at http://pubs.acs.org.

References

(1) Marčelja, S. *J. Chem. Phys.* **1974**, *60*, 3599.
(2) Dagotto, E.; Rice, T. M. *Science* **1996**, *271*, 618.
(3) (a) Waldmann, O.; Guidi, T.; Carretta, S.; Mondelli, C.; Dearden, A. L. *Phys. Rev. Lett.* **2003**, *91*, 237202. (b) Chiolero, A.; Loss, D. *Phys. Rev. Lett.* **1998**, *80*, 169.
(4) Cador, O.; Gatteschi, D.; Sessoli, R.; Larsen, F. K.; Overgaard, J.; Barra, A.-L.; Teat, S. J.; Timco, G. A.; Winpenny, R. E. P. *Angew. Chem., Int. Ed.* **2004**, *43*, 5196–5200.
(5) Taft, K. L; Delfs, C. D.; Papaefthymiou, G. C.; Foner, S.; Gatteschi, D.; Lippard, S. J. *J. Am. Chem. Soc.* **1994**, *116*, 823.
(6) Stemmler, A. J.; Kampf, J. W.; Kirk, M. L.; Atasi, B. H.; Pecoraro, V. L. *Inorg. Chem.* **1999**, *38*, 2807–2817.
(7) Geisselmann, A.; Klüfers, P.; Kropfgans, C.; Mayer, P; Piotrowski, H. *Angew. Chem., Int. Ed.* **2005**, *44*, 924–927.
(8) Grant, C. V.; Cope, W.; Ball, J. A.; Maresch, G. G.; Gaffney, B. J.; Fink, W.; Britt, R. D. *J. Phys. Chem. B* **1999**, *103*, 10627–10631.

JA9066496